Maximum Torque and Momentum Envelopes for Reaction Wheel Arrays

F. Landis Markley*
NASA's Goddard Space Flight Center, Greenbelt, MD 20771

Reid G. Reynolds†
Millennium Space Systems, Inc., Torrance, CA 90503

Frank X. Liu‡
SGT, Inc., Greenbelt, MD 20770

and

Kenneth L. Lebsock§
Orbital Sciences Corporation, Technical Services Division, Greenbelt, MD 20770

Spacecraft reaction wheel maneuvers are limited by the maximum torque and/or angular momentum that the wheels can provide. For an n-wheel configuration, the torque or momentum envelope can be obtained by projecting the n-dimensional hypercube, representing the domain boundary of individual wheel torques or momenta, into three-dimensional space via the $3\times n$ matrix of wheel axes. In this paper, the properties of the projected hypercube are discussed, and algorithms are proposed for determining this maximal torque or momentum envelope for general wheel configurations. Practical strategies for distributing a prescribed torque or momentum among the n wheels are presented, with special emphasis on a six-wheel configuration.

I. Introduction

Many spacecraft employ more than three wheels for attitude control, both for redundancy and for the additional maneuvering or momentum storage capability of the extra wheels. The Swift Gamma Ray Burst Explorer, for example, employs six reaction wheels for rapid slewing to enable observation of the initial stages of ephemeral gamma ray burst events [1], and the James Webb Space Telescope (JWST) will employ a similar reaction wheel configuration [2]. In order to employ these wheels effectively, it is necessary to characterize the maximum torque and momentum available in any direction from the reaction wheels. This knowledge is also important in designing momentum unloading strategies. For brevity of exposition, we will emphasize angular momentum in the following. Fortunately, the mathematical analysis required to identify the maximum torque capability is identical to that required for angular momentum. This analysis is the subject of this paper. Previous work on the optimal use of more than three reaction wheels has largely been limited to the four-wheel case [3, 4]. This paper is an extension of an earlier conference presentation [5].

*Aerospace Engineer, Attitude Control Systems Engineering Branch, Code 591, AIAA Fellow
† Senior GNC Engineer, Senior Member AIAA.
‡ Principal Staff Engineer; GN&C.
§ Senior Scientist, Senior Member AIAA.

In the most common case of nominally identical wheels with equal capabilities for both rotation directions, the available angular momenta fill the interior of an n-dimensional hypercube centered on the origin in reaction wheel angular momentum space. If the angular momentum capabilities vary from wheel to wheel, the angular momenta fill the interior of an n-dimensional rectangular parallelepiped in this space, where each side has length equal to twice the magnitude of the maximum angular momentum that a given wheel can provide. We will refer to this figure as a hypercube for brevity, at the expense of precision, since the case of equal wheel capabilities is the most common in practice.

The available angular momenta in three-dimensional space fill a polyhedron given by the mapping of this hypercube by the $3\times n$ reaction wheel torque distribution matrix, whose columns are the unit vectors parallel to the reaction wheel axes in three-dimensional space. We will only consider "non-defective" reaction wheel configurations, by which we mean that no three of the reaction wheel spin axis directions are coplanar. As shown below, this polyhedron is the convex hull of the mapping of the vertices of the n-dimensional hypercube, which are the points at which all n wheels are saturated in the positive or negative direction. The exterior vertices of the three-dimensional envelope are connected by edges that are the boundaries of the two-dimensional facets that form the envelope.

We have developed algorithms for defining the envelope and for finding the maximum angular momentum in a given direction. These algorithms are also adapted to determine a distribution of an arbitrary angular momentum among the wheels that minimizes the maximum of the wheel momentum magnitudes. In this minimax distribution n–2 wheels have the same maximum angular momentum magnitude, which means that the momenta lie on a scaled copy of the enveloping polyhedron whose size is determined by the required maximum wheel angular momentum magnitude rather than by the maximum wheel capability. The distribution algorithm incorporates a simple inner product test to determine which facet of the envelope gives the minimax magnitude, and hence which n–2 wheels have the maximum magnitude. It is then straightforward to find the momenta of all the wheels necessary to produce the desired net angular momentum. We consider the specific examples of configurations of three, four, five, and six reaction wheels, with emphasis on the six-wheel configuration.

II. Geometry of the Envelope

The angular momenta of an n-wheel system can be represented by an n-dimensional vector

$$\mathbf{H}_{wheels} = [H_1 \; H_2 \cdots H_n]^T \tag{1}$$

These angular momenta fill the interior of an n-dimensional hypercube, where the length of the side along the ith axis is two times the maximum angular momentum magnitude $H_{\max i}$ of the wheel along that axis. This can be the absolute maximum that the wheel can provide, or it can be some desired limiting momentum. The vertices of the hypercube are points where all wheels are saturated, i.e., they supply either their positive or negative maximum angular momenta. Each edge has all but one wheel saturated and is parallel to the axis of the unsaturated wheel. The facets of the hypercube have all but two wheels saturated.

Denoting the wheel spin axis unit vectors by $\{\hat{\mathbf{w}}_1 \; \hat{\mathbf{w}}_2 \cdots \hat{\mathbf{w}}_n\}$, the angular momentum vector in three-dimensional space is

$$\mathbf{H} = W\mathbf{H}_{wheels} \tag{2}$$

where

$$W \equiv [\hat{\mathbf{w}}_1 \; \hat{\mathbf{w}}_2 \cdots \hat{\mathbf{w}}_n] \tag{3}$$

is the angular momentum distribution matrix. The available angular momenta in three-dimensional space fill a polyhedron specified by the mapping of the n-dimensional hypercube by Eq. (2). The vertices, edges, and facets of the polyhedron in three-dimensional space are mappings of the vertices, edges, and facets of the hypercube. However, this mapping is not 1:1, since some of the vertices, edges, and facets of the hypercube will map to the interior of the polyhedron in three-dimensional space. Thus the vertices of the available polyhedron in three-dimensional space are points where all wheels are saturated. The edges of the polyhedron have all but one wheel

saturated, and an edge with wheel i unsaturated is parallel to the wheel's spin axis $\hat{\mathbf{w}}_i$. The facets have all but two wheels saturated, and the facet with wheels i and j unsaturated is a parallelogram with sides parallel to $\hat{\mathbf{w}}_i$ and $\hat{\mathbf{w}}_j$ and with normal vector in the direction of the cross product $\hat{\mathbf{w}}_i \times \hat{\mathbf{w}}_j$.

We can identify the bounding planes of the polyhedron, and thus determine the envelope, by considering all pairs i, j of wheels in turn. There are $n(n-1)/2$ such pairs for an n-wheel configuration. The i, j pair defines a set of 2^{n-2} facets of the hypercube in the n-dimensional reaction wheel command space. Each facet corresponds to a saturated command for the $n-2$ wheels other than wheels i and j, and with the angular momentum commands for wheels i and j varying over their full range over the facet. Under the transformation into three-dimensional space specified by Eq. (2), these facets map onto 2^{n-2} parallel planes with normal vector

$$\hat{\mathbf{n}}_{ij} \equiv (\hat{\mathbf{w}}_i \times \hat{\mathbf{w}}_j) \Big/ \left| \hat{\mathbf{w}}_i \times \hat{\mathbf{w}}_j \right| . \tag{4}$$

On each of these planes, the wheel angular momentum in the direction of the normal to the plane is

$$\mathbf{H} \cdot \hat{\mathbf{n}}_{ij} = \sum_{k=1}^{n} H_k (\hat{\mathbf{w}}_k \cdot \hat{\mathbf{n}}_{ij}) = \sum_{k \neq i,j} \sigma_k H_{\max k} (\hat{\mathbf{w}}_k \cdot \hat{\mathbf{n}}_{ij}) , \tag{5}$$

where $\sigma_k = \pm 1$ specifies the direction of saturation of the angular momentum on wheel k. Wheels i and j can clearly be omitted from the sum, since they don't contribute to the angular momentum perpendicular to the plane. This is indicated algebraically by the vanishing of the triple product $\hat{\mathbf{w}}_k \cdot (\hat{\mathbf{w}}_i \times \hat{\mathbf{w}}_j)$ for $k = i$ or j. This triple product does not vanish for any other k, since we have assumed a "non-defective" reaction wheel configuration, for which no three of the reaction wheel spin axis directions are coplanar.

The planes with the maximum and minimum angular momentum in the direction of the normal are the planes for which

$$\sigma_k = \text{sign}[\hat{\mathbf{w}}_k \cdot (\hat{\mathbf{w}}_i \times \hat{\mathbf{w}}_j)] = \text{sign}(\hat{\mathbf{w}}_k \cdot \hat{\mathbf{n}}_{ij}) \tag{6a}$$

or

$$\sigma_k = -\text{sign}[\hat{\mathbf{w}}_k \cdot (\hat{\mathbf{w}}_i \times \hat{\mathbf{w}}_j)] = -\text{sign}(\hat{\mathbf{w}}_k \cdot \hat{\mathbf{n}}_{ij}) \tag{6b}$$

for all k other than i and j. It is clear that these two planes and only these of the 2^{n-2} parallel planes for the i, j pair form part of the angular momentum envelope. On each of these bounding facets H_i and H_j vary over the range between $\pm H_{\max i}$ and $\pm H_{\max j}$, respectively. Saturation of H_i and H_j give the four corners of a parallelogram, so we can identify eight of the vertices of the envelope for each i, j pair, corresponding to the two signs each for saturated H_i and H_j, and the overall sign of the other saturated wheel angular momenta given by Eq. (6a) or (6b).

Carrying out the above procedure over all pairs i, j will produce a total of $4n(n-1)$ vertices. These aren't all distinct, however, for each vertex will be identified once for each bounding plane of the envelope that intersects there. This is useful information about the "structure" of the envelope, where "structure" denotes the number of vertices of the envelope, and the number of planes and edges that intersect at each vertex, as well as the specific information about which wheels are saturated in which direction at each vertex. It is interesting that this structure depends only on the unit vectors through their triple products $\hat{\mathbf{w}}_k \cdot (\hat{\mathbf{w}}_i \times \hat{\mathbf{w}}_j)$, and not on the maximum angular momentum capabilities of the wheels. If this angular momentum capability is changed, the shape of the envelope will change, but not the structure as defined here. It is obvious that the envelope has an inversion symmetry; for each point on the envelope with angular momentum $\mathbf{H}$ there is a corresponding point with angular momentum $-\mathbf{H}$ obtained by reversing all the wheel momenta.

We will assume for the remainder of the paper that all the $H_{\max i}$ are equal, so we can omit the subscript i on $H_{\max}$. We also avoid the use of Eq. (6b) by distinguishing between the ij facet and the ji facet and always using Eq. (6a). Then on the ij facet of the polyhedron the wheel momentum is

$$\mathbf{H} = H_i \hat{\mathbf{w}}_i + H_j \hat{\mathbf{w}}_j + H_{\max} \sum_{k \neq i,j} \hat{\mathbf{w}}_k \text{sign}(\hat{\mathbf{w}}_k \cdot \hat{\mathbf{n}}_{ij}) = H_i \hat{\mathbf{w}}_i + H_j \hat{\mathbf{w}}_j + H_{\max} \mathbf{v}_{ij} , \tag{7}$$

where

$$\mathbf{v}_{ij} \equiv \sum_{k \neq i,j} \hat{\mathbf{w}}_k \text{sign}(\hat{\mathbf{w}}_k \cdot \hat{\mathbf{n}}_{ij}). \tag{8}$$

The wheel momentum in the direction of the normal to the facet is

$$H_{ij} \equiv \mathbf{H} \cdot \hat{\mathbf{n}}_{ij} = H_{\max}(\mathbf{v}_{ij} \cdot \hat{\mathbf{n}}_{ij}) = H_{\max} d_{ij}, \tag{9}$$

where

$$d_{ij} \equiv \mathbf{v}_{ij} \cdot \hat{\mathbf{n}}_{ij} = \sum_{k \neq i,j} \left| \hat{\mathbf{w}}_k \cdot \hat{\mathbf{n}}_{ij} \right|. \tag{10}$$

If the vector $H_{ij}\hat{\mathbf{n}}_{ij}$ ends at a point on the bounding polyhedron, then H_{ij} is the minimum angular momentum capability on that facet. This is not guaranteed to be the case, however, as we will show in Section V of this paper. It is always true, though, that the minimum value of H_{ij} over all the facets is the minimum angular momentum capability of the reaction wheel configuration.

III. Optimizing the Angular Momentum Commands

A. Optimality Criterion

Optimal use of the angular momentum capability of a wheel configuration requires that equal demands be made on all wheels. In the case of wheels with identical capacities, this is accomplished by minimizing the maximum value, or L_∞ norm, of the set of individual wheel angular momenta that will produce the desired net angular momentum. This minimax value H_0, which must be determined, determines the angular momentum envelope, as in the previous section, and the required angular momentum commands; it clearly cannot exceed the wheel capability of any wheel. The generalization to wheel assemblies with varying capabilities is straightforward, but we will not consider this uncommon case.

B. Numerical Algorithm For Finding The L_∞ Momentum Distribution

Finding the L_∞ momentum distribution requires identifying the facet of the wheel envelope that contains a point along the desired angular momentum axis. Assuming that we have found this to be facet *ij*, we write Eq. (7) as

$$\mathbf{H} = [\hat{\mathbf{w}}_i \ \hat{\mathbf{w}}_j \ \mathbf{v}_{ij}][H_i \ H_j \ H_0]^T, \tag{11}$$

where $H_{\max}$, the maximum allowed momentum, has been replaced by H_0, the maximum momentum for this particular value of **H**. Equation (11) can be solved to give the wheel momenta as

$$H_i = [\mathbf{v}_{ij} \cdot (\hat{\mathbf{w}}_i \times \hat{\mathbf{w}}_j)]^{-1}[(\hat{\mathbf{w}}_j \times \mathbf{v}_{ij}) \cdot \mathbf{H}] \tag{12a}$$

$$H_j = [\mathbf{v}_{ij} \cdot (\hat{\mathbf{w}}_i \times \hat{\mathbf{w}}_j)]^{-1}[(\mathbf{v}_{ij} \times \hat{\mathbf{w}}_i) \cdot \mathbf{H}] \tag{12b}$$

$$H_0 = \mathbf{w}_{ij} \cdot \mathbf{H}, \tag{12c}$$

where

$$\mathbf{w}_{ij} \equiv d_{ij}^{-1} \hat{\mathbf{n}}_{ij}. \tag{13}$$

Note that the vectors $\mathbf{v}_{ji}$ and $\mathbf{w}_{ji}$ are not unit vectors, and that $\mathbf{v}_{ji} = -\mathbf{v}_{ij}$ and $\mathbf{w}_{ji} = -\mathbf{w}_{ij}$. The individual wheel angular momenta for $k \neq i, j$ are

$$H_k = H_0 \, \text{sign}(\hat{\mathbf{w}}_k \cdot \mathbf{w}_{ij}) \quad \text{for} \quad k \neq i, j. \tag{14}$$

We can avoid cross-product computations by using the identity

$$\left|\hat{\mathbf{w}}_i \times \hat{\mathbf{w}}_j\right|^2 \mathbf{v}_{ij} = [\hat{\mathbf{w}}_i \cdot \mathbf{v}_{ij} - (\hat{\mathbf{w}}_i \cdot \hat{\mathbf{w}}_j)(\hat{\mathbf{w}}_j \cdot \mathbf{v}_{ij})]\hat{\mathbf{w}}_i + [\hat{\mathbf{w}}_j \cdot \mathbf{v}_{ij} - (\hat{\mathbf{w}}_i \cdot \hat{\mathbf{w}}_j)(\hat{\mathbf{w}}_i \cdot \mathbf{v}_{ij})]\hat{\mathbf{w}}_j + [(\hat{\mathbf{w}}_i \times \hat{\mathbf{w}}_j) \cdot \mathbf{v}_{ij}](\hat{\mathbf{w}}_i \times \hat{\mathbf{w}}_j) \quad (15)$$

to rewrite Eqs. (12a) and (12b) as

$$H_i = \left|\hat{\mathbf{w}}_i \times \hat{\mathbf{w}}_j\right|^{-2} [\hat{\mathbf{w}}_i \cdot \mathbf{H} - (\hat{\mathbf{w}}_i \cdot \hat{\mathbf{w}}_j)(\hat{\mathbf{w}}_j \cdot \mathbf{H}) - c_{ij} H_0] \quad (16a)$$

$$H_j = \left|\hat{\mathbf{w}}_i \times \hat{\mathbf{w}}_j\right|^{-2} [\hat{\mathbf{w}}_j \cdot \mathbf{H} - (\hat{\mathbf{w}}_i \cdot \hat{\mathbf{w}}_j)(\hat{\mathbf{w}}_i \cdot \mathbf{H}) + c_{ji} H_0], \quad (16b)$$

where

$$c_{ij} \equiv \hat{\mathbf{w}}_i \cdot \mathbf{v}_{ij} - (\hat{\mathbf{w}}_i \cdot \hat{\mathbf{w}}_j)(\hat{\mathbf{w}}_j \cdot \mathbf{v}_{ij}) = (\hat{\mathbf{w}}_i \times \hat{\mathbf{w}}_j) \cdot (\mathbf{v}_{ij} \times \hat{\mathbf{w}}_j). \quad (17)$$

If the vectors $\mathbf{w}_{ij}$ and the scalars $\left|\hat{\mathbf{w}}_i \times \hat{\mathbf{w}}_j\right|^{-2}$ and c_{ij} for all the facets are precomputed and stored onboard along with the wheel axis unit vectors, the wheel angular momentum computations require only dot products, multiplications, and additions.

The equations relating $\mathbf{H}_{wheels}$ to $\mathbf{H}$ are linear, so the mapping for facet *ij* can equivalently be written in matrix form as

$$\mathbf{H}_{wheels} = W_{ij}^* \mathbf{H}. \quad (18)$$

Each matrix W_{ij}^* is a right inverse of *W*, meaning that their product is the 3×3 identity matrix; $WW_{ij}^* = I_{3\times 3}$. These matrices can be pre-computed, and inspection of Eqs. (12)–(14) reveals that $W_{ij}^* = W_{ji}^*$, so it is only necessary to compute and store one matrix for each pair of parallel facets in this formulation.

C. Finding the Correct Facet

If the computations of Eq. (12) yield a solution with either H_i or H_j having magnitude greater than H_0, it means that the *ij* facet is not the facet that gives the minimax momentum distribution. We now demonstrate a simple dot product test for finding the correct facet before performing these computations. Suppose the momentum vector **H** points to facet f_{ij}, as shown in Figure 1. The normal vector $\hat{\mathbf{n}}_{ij}$ to the facet f_{ij} and the momentum vector **H**, and thus the triangle *OAG*, lie in the plane of the figure. Consider any other facet f_{kl} whose normal is less than 90° from **H**. The normal vector $\hat{\mathbf{n}}_{kl}$ to this facet is not in the plane of the figure in general, and thus only the edge *OF* of the triangle *OFE* is guaranteed to be in the plane of the figure. The blue lines in Figure 1 are out of the plane of the paper. The lengths |*OA*| and |*OB*| are given by

$$|OA| = H_{ij} = H_{\max} d_{ij} \quad (19a)$$

$$|OB| = \hat{\mathbf{n}}_{ij} \cdot \mathbf{H}, \quad (19b)$$

using Eq. (9) for H_{ij}, the distance of facet f_{ij} from the origin. The convexity of the momentum polyhedron means that $|OF| \geq |OG|$ and therefore

$$\frac{\mathbf{w}_{kl} \cdot \mathbf{H}}{H_{\max}} = \frac{\hat{\mathbf{n}}_{kl} \cdot \mathbf{H}}{H_{kl}} = \frac{|OD|}{|OE|} = \frac{|OC|}{|OF|} \leq \frac{|OC|}{|OG|} = \frac{|OB|}{|OA|} = \frac{\hat{\mathbf{n}}_{ij} \cdot \mathbf{H}}{H_{ij}} = \frac{\mathbf{w}_{ij} \cdot \mathbf{H}}{H_{\max}}. \quad (20)$$

Equation (13) has been used for the outer terms in this inequality, which show that the correct facet is the one with the maximum value of $\mathbf{w}_{ij} \cdot \mathbf{H}$. The equality of W_{ij}^* and W_{ji}^* means that we only have to identify the correct pair of parallel facets, and the relation $\mathbf{w}_{ji} = -\mathbf{w}_{ij}$ tells us that this is equivalent to finding the maximum value of $\left|\mathbf{w}_{ij} \cdot \mathbf{H}\right|$.

D. L_2 Alternative

For comparative purposes, we consider the L_2 alternative to the L_∞ analysis emphasized in this paper. The L_2 norm minimizes the sum of the squares of the wheel momenta, rather than the maximum wheel momentum. It is well known that the wheel momentum distribution minimizing the L_2 norm is given by [6]

$$\mathbf{H}_{wheels} = W^{+}\mathbf{H}, \tag{21}$$

where W^{+} is the Moore-Penrose pseudoinverse of W, which is given in this case by

$$W^{+} = W^{T}(WW^{T})^{-1}. \tag{22}$$

Equation (21) will almost always result in the momentum of at of least one wheel having a greater magnitude than would result from Eq. (18).

IV. Specific Cases

We will consider four specific cases. The first three are symmetric configurations of three, four, and six wheels, respectively, with the wheel spin axes all at an angle η from the yz plane, and uniformly distributed in azimuth about the x axis. The fourth case we will consider is the asymmetrical five-wheel case resulting from deletion of one wheel from the six-wheel configuration. The momentum envelopes for these four configurations are shown for comparison in Figures 2-5. The unit of length in these figures is the maximum angular momentum capability of a single wheel. The torque envelope, scaled to the maximum torque capability of a single wheel, is identical. Since the figures represent both envelopes, they are labeled Envelope, rather than Torque Envelope or Momentum Envelope. They all have the same elevation angle $\eta = 35.26°$, which was chosen because it results in the largest minimum dimension of each of the envelopes, i.e. closest to spherical shape, as we will show algebraically below. For purpose of comparison, the four figures are all drawn to the same scale, viewed from the same vantage point, and have the same illumination sources. In a practical case for a specific mission, the choice of the angle η is based on some compromise among convenience of fabrication, expected momentum accumulation, slewing requirements, and spacecraft inertia properties.

A. 3-Wheel Configuration

First consider the easy case of three wheels, with

$$W = \begin{bmatrix} s & s & s \\ 0 & \frac{\sqrt{3}}{2}c & -\frac{\sqrt{3}}{2}c \\ c & -\frac{1}{2}c & -\frac{1}{2}c \end{bmatrix}, \tag{23}$$

where $s \equiv \sin\eta$ and $c \equiv \cos\eta$. In this case, there is no distinction between the L_∞ and L_2 norms. The wheel momenta are given uniquely by the relation

$$\mathbf{H}_{wheels} = W^{-1}\mathbf{H}, \tag{24}$$

which of necessity minimizes both norms. The structure of the envelope is that of a cube, with three planes meeting at each vertex. Thus each vertex will be identified three times by the procedure described above, and the number of distinct vertices is $4\cdot3\cdot(3–1)/3 = 8$, the correct number of vertices of a cube.

The maximum storage capacity on the 12 facet is found by computing

$$\hat{\mathbf{w}}_1 \times \hat{\mathbf{w}}_2 = \frac{c}{2}\begin{bmatrix} -\sqrt{3}\,c \\ 3s \\ \sqrt{3}\,s \end{bmatrix} \tag{25}$$

and

$$d_{12} = \frac{3cs}{\sqrt{1+3s^2}}. \tag{26}$$

The storage on all the other facets is the same in this simple case. The storage as a function of η is maximized for

$$\eta = \sin^{-1}\left(\tfrac{1}{\sqrt{3}}\right) = \tfrac{1}{2}\cos^{-1}\left(\tfrac{1}{3}\right) = 35.26°, \tag{27}$$

which gives $d_{12} = 1$. For this value of η, the axes are all perpendicular, so the momentum or torque envelope has the form of a tilted cube, as illustrated in Figure 2. It is not surprising that the minimum storage capacity for orthogonal wheel axes is the capacity of one wheel. It would be more common practice to orient three wheel axes along the spacecraft axes, in which case the wheel distribution matrix W would be the 3×3 identity matrix and the cube edges would be parallel to the x, y, and z axes. The magnitude of the minimum momentum or torque capability does not depend on the orientation of the cube.

B. 4-Wheel Configuration

We next consider the often-employed case of four reaction wheels oriented in a tetrahedral configuration around the x axis. The angular momentum distribution matrix is

$$W = \begin{bmatrix} s & s & s & s \\ 0 & c & 0 & -c \\ c & 0 & -c & 0 \end{bmatrix}, \tag{28}$$

This four-wheel configuration has an envelope with 14 vertices. Six of the vertices are defined by the intersection of four facets each and 8 by three facets each. The torque or momentum envelope for this configuration, again assuming identical wheels, is shown in Figure 3. This envelope has a fourfold rotational symmetry about the x axis, which is the vertical axis in the figure.

We now want to determine the storage capacity of the four-wheel configuration. In this case, there are only two different types of facet. Consider first the 12 facet.

$$\hat{\mathbf{w}}_1 \times \hat{\mathbf{w}}_2 = c \begin{bmatrix} -c \\ s \\ s \end{bmatrix} \tag{29}$$

so

$$d_{12} = \frac{4cs}{\sqrt{1+s^2}}. \tag{30}$$

The coefficients d_{ij} for facets 23, 34, 41, 21, 32, 43, and 14 are the same.

Now consider the 13 facet.

$$\hat{\mathbf{w}}_1 \times \hat{\mathbf{w}}_3 = 2cs \begin{bmatrix} 0 \\ 1 \\ 0 \end{bmatrix} \tag{31}$$

so

$$d_{13} = 2c. \tag{32}$$

The coefficients d_{ij} for facets 24, 31, and 42 are the same. The storage as a function of η is maximized at the angle that gives $d_{12} = d_{13}$, which is $\eta = 35.26°$, the same value that maximizes storage in the three-wheel case. For this value of η, the ratio of the minimum momentum storage to the capacity of a single wheel is $d_{12} = d_{13} = \sqrt{8/3} = 1.633$.

C. 6-Wheel Configuration

The next case we consider has the wheels oriented with hexagonal symmetry around the x axis. The angular momentum distribution matrix is

$$W = \begin{bmatrix} s & s & s & s & s & s \\ 0 & \frac{\sqrt{3}}{2}c & \frac{\sqrt{3}}{2}c & 0 & -\frac{\sqrt{3}}{2}c & -\frac{\sqrt{3}}{2}c \\ c & \frac{1}{2}c & -\frac{1}{2}c & -c & -\frac{1}{2}c & \frac{1}{2}c \end{bmatrix}. \tag{33}$$

This six-wheel configuration has an envelope with 32 vertices. Two of the vertices are defined by the intersection of six facets each, 18 by four facets each, and 12 by three facets each. Figure 4 illustrates the torque or momentum envelope for six wheels with identical capabilities in this configuration. This envelope has a sixfold rotational symmetry about the x axis. This is the reaction wheel configuration on the Swift or JWST spacecraft, except that the symmetry axis of the JWST wheel configuration is the z axis rather than the x axis.

We now want to look at the special six-wheel instance of the general vector relations derived above. As we have seen, there are only three different types of facet. Consider first the 12 facet.

$$\hat{\mathbf{w}}_1 \times \hat{\mathbf{w}}_2 = \frac{c}{2}\begin{bmatrix} -\sqrt{3}\,c \\ s \\ \sqrt{3}\,s \end{bmatrix} \tag{34}$$

so

$$d_{12} = \frac{6\sqrt{3}\,cs}{\sqrt{3+s^2}}. \tag{35}$$

The coefficients d_{ij} for facets 23, 34, 45, 56, 61, 21, 32, 43, 54, 65, and 16 are the same.

Now consider the 13 facet.

$$\hat{\mathbf{w}}_1 \times \hat{\mathbf{w}}_3 = \frac{c}{2}\begin{bmatrix} -\sqrt{3}\,c \\ 3s \\ \sqrt{3}\,s \end{bmatrix} \tag{36}$$

so

$$d_{13} = \frac{8\,cs}{\sqrt{1+3s^2}}. \tag{37}$$

The coefficients d_{ij} for facets 24, 35, 46, 51, 62, 31, 42, 53, 64, 15, and 26 are the same.

We finally consider the 14 facet.

$$\hat{\mathbf{w}}_1 \times \hat{\mathbf{w}}_4 = 2cs\begin{bmatrix} 0 \\ 1 \\ 0 \end{bmatrix} \tag{38}$$

so

$$d_{14} = 2\sqrt{3}\,c\ . \tag{39}$$

The coefficients d_{ij} for facets 25, 36, 41, 52, and 63 are the same.

The c_{ij} coefficients defined by Eq. (17) are

$$c_{12} = c_{23} = c_{34} = c_{45} = c_{56} = c_{61} = -c_{21} = -c_{32} = -c_{43} = -c_{54} = -c_{65} = -c_{16} = (1/4)c^2(3-11s^2) \tag{40a}$$

$$c_{13} = c_{24} = c_{35} = c_{46} = c_{51} = c_{62} = -c_{13} = -c_{42} = -c_{53} = -c_{64} = -c_{15} = -c_{26} = (3/4)c^2(3-7s^2) \tag{40b}$$

$$c_{14} = c_{25} = c_{36} = c_{41} = c_{52} = c_{63} = 0\,. \tag{40c}$$

For the JWST angle $\eta = 30°$, we have $d_{12} = 2.4962$, $d_{13} = 2.6186$, $d_{14} = 3$, $c_{12} = 3/64$ and $c_{13} = 45/64$. The minimum storage could be maximized by choosing η to maximize d_{13}. This maximum is at $\eta = 35.26°$ in this case, as in the three and four-wheel cases, which gives $d_{12} = 6/\sqrt{5} = 2.683$, $d_{13} = 8/3 = 2.667$, $d_{14} = 2\sqrt{2} = 2.828$, $c_{12} = -1/9$ and $c_{13} = 1/3$. The optimal η gives a polyhedron that approximates a sphere as closely as possible, but it provides less than 7% more capacity in the worst direction than $\eta = 30°$ does.

D. 5-Wheel Configuration

We will not consider a symmetric configuration of five wheels, but rather the asymmetric configuration resulting from the failure of one wheel from the symmetric six-wheel configuration. Figure 5 shows the torque or momentum envelope for the case where the angular momentum distribution matrix is obtained by deleting one column from the matrix of Eq. (33).

There are six different types of facets in the failed wheel cases. We will only consider the case that wheel 6 has failed; the other cases can be found easily by permutation of indices. In this case

$$d_{12} = d_{21} = d_{45} = d_{54} = \frac{5\sqrt{3}\,cs}{\sqrt{3+s^2}} \tag{41a}$$

$$d_{13} = d_{31} = d_{35} = d_{53} = \frac{6\,cs}{\sqrt{1+3s^2}} \tag{41b}$$

$$d_{14} = d_{41} = d_{25} = d_{52} = \frac{3\sqrt{3}\,c}{2} \tag{41c}$$

$$d_{23} = d_{32} = d_{34} = d_{43} = \frac{4\sqrt{3}\,cs}{\sqrt{3+s^2}} \tag{41d}$$

$$d_{15} = d_{51} = \frac{7cs}{\sqrt{1+3s^2}} \tag{41e}$$

$$d_{24} = d_{42} = \frac{5cs}{\sqrt{1+3s^2}} \tag{41f}$$

For the wheel inclination angle that gives the maximum momentum storage in the worst direction, $\eta = 35.26°$, the smallest of these is $d_{24} = d_{42}$, and it has just 5/8 of the smallest value for the full six-wheel configuration. It is no longer generally true that $c_{ij} = -c_{ji}$ in the failed wheel case. For example, we find that $c_{14} = 3c^2s^2$ and $c_{41} = -c^2s^2$ if wheel 6 has failed.

V. More on the Geometry of the Envelope

The *ij* facet is a parallelogram with sides parallel to $\hat{\mathbf{w}}_i$ and $\hat{\mathbf{w}}_j$. This is a subset, defined by the conditions that $|H_i| \le H_0$ and $|H_j| \le H_0$, of an infinite plane. The point on this extended plane that is closest to the origin is the point where an angular momentum normal to the plane would lie. We want to find out whether this point lies on the facet, which we noted below Eq. (10) to not always be the case. Equations (16a) and (16b) show that $H_i = -\left|\hat{\mathbf{w}}_i \times \hat{\mathbf{w}}_j\right|^{-2} c_{ij} H_0$ and $H_j = \left|\hat{\mathbf{w}}_i \times \hat{\mathbf{w}}_j\right|^{-2} c_{ji} H_0$ if $\mathbf{H}$ is normal to the plane. Thus the conditions that the normal point lies on the facet are $|c_{ij}| \le \left|\hat{\mathbf{w}}_i \times \hat{\mathbf{w}}_j\right|^2$ and $|c_{ji}| \le \left|\hat{\mathbf{w}}_i \times \hat{\mathbf{w}}_j\right|^2$.

For the six-wheel configurations, it is clear that the six facets described by Eq. (40c) contain their normal points for any wheel elevation angle. The twelve facets described by Eqs. (34) and (40a) contain their normal points only if

$s^2 \le 1/2$ or $\eta \le 45°$. The twelve facets described by Eqs. (36) and (40b) contain their normal points only if $s^2 \ge 1/5$ or $\eta \ge 26.565°$. In the range $26.565° \le \eta \le 45°$ all the vectors $H_{ij}\hat{\mathbf{n}}_{ij}$ end on the bounding polyhedron.

In the five-wheel configurations, not all of the vectors $H_{ij}\hat{\mathbf{n}}_{ij}$ end on the bounding polyhedron even for $\eta = 30°$ or $\eta = 35.26°$.

VI. Avoiding Equal Wheel Speeds

It is often undesirable to have multiple wheels running at the same speed, so in the case of $n > 3$ wheels we can use vectors in the (n–3)-dimensional null space of W to separate the wheels speeds. Angular momentum commands in the null space can also be used to drive a wheel's speed rapidly through zero or past the frequency of a flexible mode of the spacecraft structure without perturbing the pointing of the spacecraft.

The null space is one-dimensional in four-wheel case, so all null vectors are multiples of

$$\mathbf{p} = \tfrac{1}{2}[1 \quad -1 \quad 1 \quad -1]^T . \tag{42}$$

Even though there is only one null vector, the L_∞ algorithm assigns momenta on every facet with signs that enable this null vector to separate any equal wheel speeds.

Several convenient null vectors in the six-wheel case are:

$$\mathbf{u}_0 = \tfrac{1}{\sqrt{6}}[1 \quad -1 \quad 1 \quad -1 \quad 1 \quad -1]^T \tag{43a}$$

$$\mathbf{u}_{14} = \tfrac{1}{2}[0 \quad 1 \quad -1 \quad 0 \quad 1 \quad -1]^T \tag{43b}$$

$$\mathbf{u}_{25} = \tfrac{1}{2}[-1 \quad 0 \quad 1 \quad -1 \quad 0 \quad 1]^T \tag{43c}$$

$$\mathbf{u}_{36} = \tfrac{1}{2}[1 \quad -1 \quad 0 \quad 1 \quad -1 \quad 0]^T \tag{43d}$$

$$\mathbf{u}_1 = \tfrac{1}{6}[0 \quad 1 \quad -3 \quad 4 \quad -3 \quad 1]^T \tag{43e}$$

$$\mathbf{u}_2 = \tfrac{1}{6}[1 \quad 0 \quad 1 \quad -3 \quad 4 \quad -3]^T \tag{43f}$$

$$\mathbf{u}_3 = \tfrac{1}{6}[-3 \quad 1 \quad 0 \quad 1 \quad -3 \quad 4]^T \tag{43g}$$

$$\mathbf{u}_4 = \tfrac{1}{6}[4 \quad -3 \quad 1 \quad 0 \quad 1 \quad -3]^T \tag{43h}$$

$$\mathbf{u}_5 = \tfrac{1}{6}[-3 \quad 4 \quad -3 \quad 1 \quad 0 \quad 1]^T \tag{43i}$$

$$\mathbf{u}_6 = \tfrac{1}{6}[1 \quad -3 \quad 4 \quad -3 \quad 1 \quad 0]^T \tag{43j}$$

The indices indicate the locations of zeros in the vectors. The normalization factors are chosen to give unit vectors, but they're really irrelevant because there's no requirement for the null space vectors to be normalized. Note that $\mathbf{u}_{14} + \mathbf{u}_{25} + \mathbf{u}_{36} = \mathbf{0}$ and that $\mathbf{u}_0$ is orthogonal to $\mathbf{u}_{14}$, $\mathbf{u}_{25}$, and $\mathbf{u}_{36}$.

In the six-wheel case, $\mathbf{u}_0$ and any two of $\mathbf{u}_{14}$, $\mathbf{u}_{25}$, or $\mathbf{u}_{36}$ constitute a basis for the three-dimensional null space. The failed wheel cases are equally simple. In the case of a failed wheel 6, for example, $\mathbf{u}_6$ and $\mathbf{u}_{36}$ constitute an orthogonal basis for the two-dimensional null space. The other failed wheel cases are similar.

An alternative method of avoiding wheels running at the same speed is to distribute the momenta according to a blend of the L_∞ and L_2 distribution laws,

$$\mathbf{H}_{wheels} = (1-k)W_{ij}^{*}\mathbf{H} + kW^{+}\mathbf{H} , \tag{44}$$

where k is a scalar constant between 0 and 1. Choosing the smallest value of k that gives an acceptable separation of wheel speeds maximizes the momentum storage capacity. This alternative is really a special case of using vectors in the null space to separate the wheel speeds, because all the columns of $W_{ij}^{*} - W^{+}$ lie in the null space.

VII. Slews

A slew can be executed under reaction wheel control by varying the total reaction wheel momentum vector in three-dimensional space according to some slew law specifying a torque $\dot{\mathbf{H}}$. The L_∞ distribution of this torque among the reaction wheels is given in analogy with Eq. (18) by

$$\dot{\mathbf{H}}_{wheels} = W_{ij}^{*}\dot{\mathbf{H}}, \tag{45}$$

where the ij facet is the one with the maximum value of $\mathbf{w}_{ij} \cdot \dot{\mathbf{H}}$. Note that this torque will not necessarily keep the reaction wheels in a state that minimizes the L_∞ norm of their momenta, because the facet on which $\mathbf{w}_{ij} \cdot \dot{\mathbf{H}}$ is maximized is not the same as the facet on which $\mathbf{w}_{ij} \cdot \mathbf{H}$ is maximized, in general. This can be dealt with by setting up reaction wheel control loops to feedforward the L_∞ torque and then to use tachometer feedback to asymptotically drive the wheels to the L_∞ momentum distribution. These loops can be incorporated into a wheel drag compensation loop as illustrated schematically in Figure 6.

Another option is to maintain the L_∞ momentum distribution by commanding the wheel torques to be the derivatives of the momenta computed by Eq. (18). This protects against momentum saturation of the wheels and is easier to implement, but it gives discontinuous wheel torque commands when the momentum moves from one facet of the polyhedron to another, and it will generally result in larger wheel torque commands than those computed by Eq. (45). Spacecraft requirements differ, and the desire to minimize wheel momentum must be balanced against the desire to minimize wheel torques for any given application. Generally speaking, the time required to execute small slews tends to be dominated by the torque capability of the reaction wheels, and the time for large slews by the momentum capacity of the wheels.

The L_2 distribution law does not have this complication; taking the derivative Eq. (21) gives

$$\dot{\mathbf{H}}_{wheels} = W^{+}\dot{\mathbf{H}}, \tag{46}$$

because the pseudoinverse is a constant matrix. Thus applying torques distributed according to an L_2 law will preserve an L_2 momentum distribution.

VIII. Conclusions

We have presented algorithms for determining the envelope of available torques and angular momenta in three-dimensional space for general configurations of n reaction wheels. These fill a polyhedron given by projection into three-dimensional space of an n-dimensional hypercube in reaction wheel space. This polyhedron is the convex hull of the projection of the vertices of the hypercube, the points at which all the wheels are saturated in the positive or negative direction. We have also presented an algorithm for finding the optimal angular momentum commands to produce any desired angular momentum. The optimality criterion is that these commands minimize the maximum value, or L_∞ norm, of the vector of individual wheel angular momenta. The algorithm also determines the maximum angular momentum available in any given direction. The exact solution algorithm is computationally feasible for onboard processing, especially if the necessary quantities for a specific wheel configuration are precomputed. The onboard computations could be further reduced by storing the maps of vector angular momentum or torque to individual wheels as a set of $n \times 3$ matrices, one for each pair of opposite facets, at the cost of greater onboard computer storage.

Acknowledgements

We would like to acknowledge helpful contributions from Peiman Maghami, Roger Chen, Satya Anandakrishnan, Chunlei Rui, Henry Fu, and Nicholas Rubi.

References

[1] http://swift.sonoma.edu/

[2] http://www.jwst.nasa.gov/

[3] Kawaguchi, J., Maeda, K., Matsuo, H., and Ninomiya, K., "Closed Loop Momentum Transfer Maneuvers Using Multiwheels," *Journal of Guidance, Control, and Dynamics*, Vol. 18, No. 4, July-Aug. 1995, pp. 867-874.

[4] Steyn, W. H., "Near-Minimum-Time Eigenaxis Rotation Maneuvers Using Reaction Wheels," *Journal of Guidance, Control, and Dynamics*, Vol. 18, No. 5, Sept-Oct. 1995, pp. 1184-1189.

[5] Reynolds , R. G., and Markley, F. L., "Maximal Torque and Momentum Envelopes for Reaction Wheel Arrays," Flight Mechanics Symposium, Goddard Space Flight Center, Greenbelt, MD, June 2001, NASA Conference Publication NASA/CP-2001-209986, pp. 327–334.

[6] Golub, G. H. and Van Loan, C. F., *Matrix Computations*, p. 139, The Johns Hopkins University Press, Baltimore, MD, 1983, pp. 186, 187.

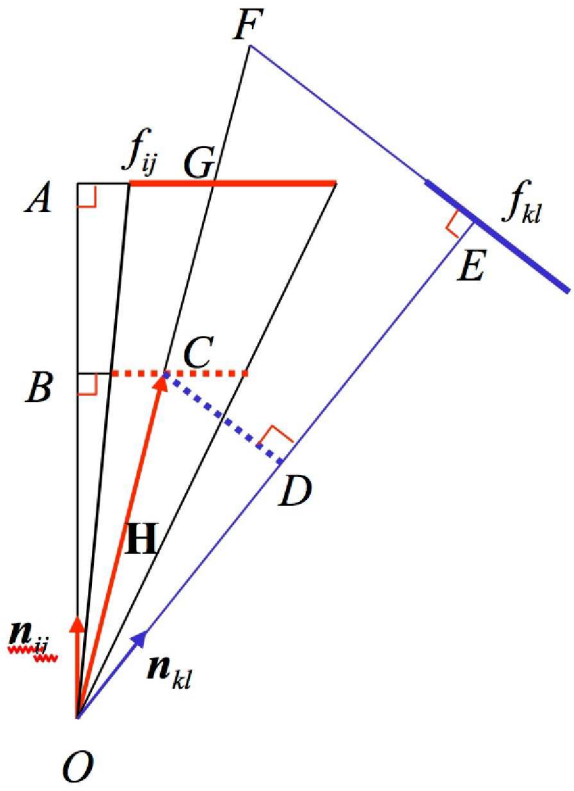

Figure 1. Finding the Correct Facet

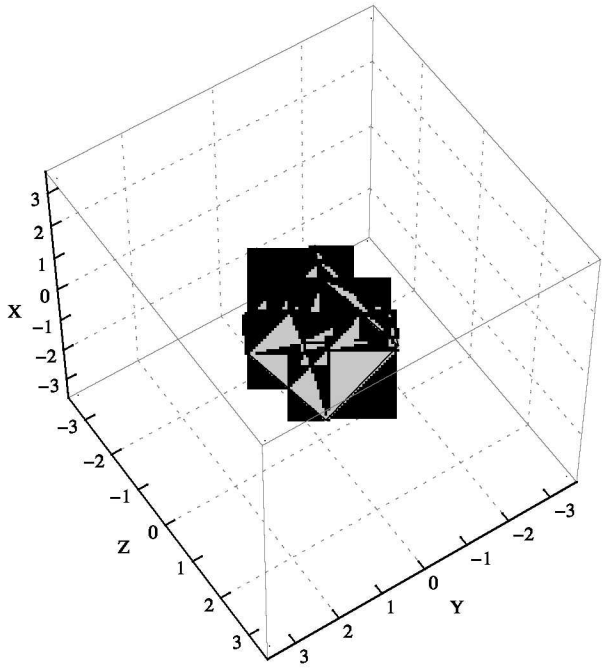

Figure 2. Three Orthogonal Wheel Configuration Envelope

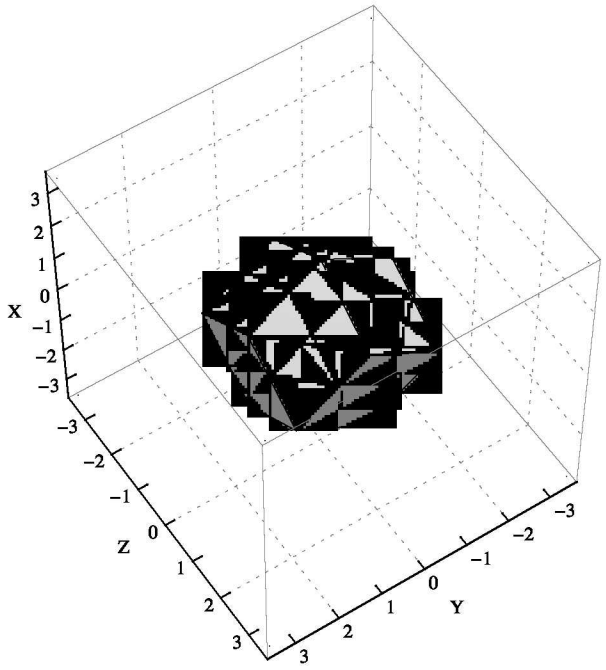

Figure 3. Four Symmetric Wheel Configuration Envelope

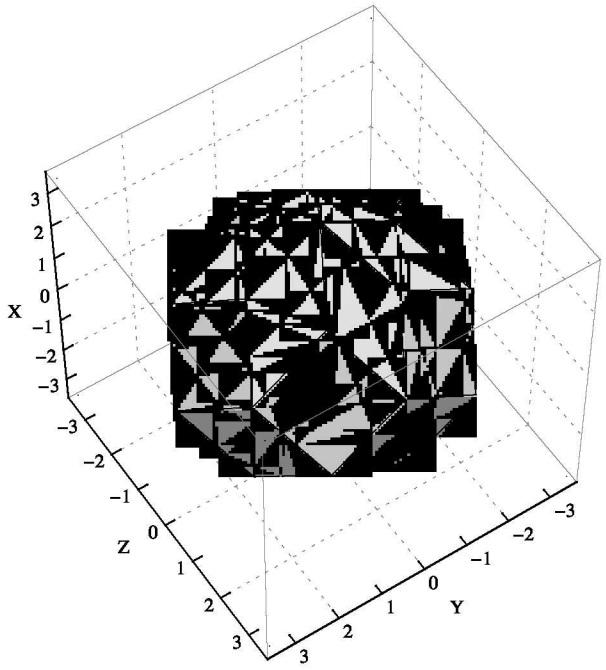

Figure 4. Six Symmetric Wheel Configuration Envelope

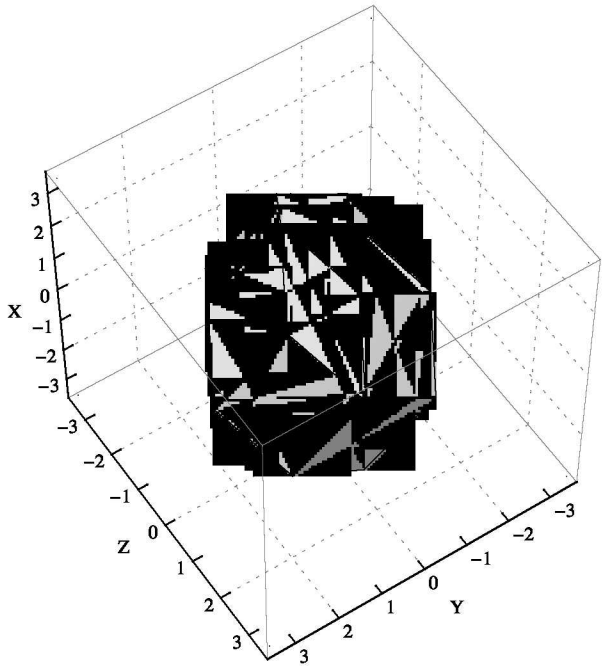

Figure 5. Envelope of Six-Wheel Configuration with One Wheel Failed

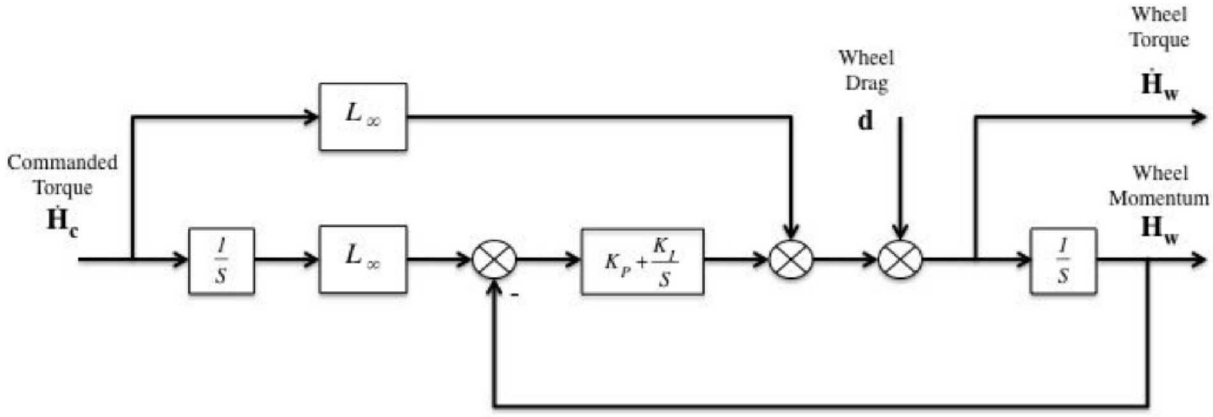

Figure 6. Combined Torque and Momentum Control Loops